Transceiver polarization power imbalance compensation and monitoring for coherent digital subcarrier modulation system

Linsheng Fan[1] , Yanfu Yang[1,*] , Chen Cheng[1] , Yaguang Hao[1] , Yong Yao[1]
[1]Department of Electronic and Information Engineering, Harbin Institute of Technology, Shenzhen 518055, China
e-mail: yangyanfu@hit.edu.cn

***Abstract*— A transceiver polarization power imbalance compensation and monitoring scheme using frequency pilots for coherent digital subcarrier modulation system is proposed and demonstrated experimentally. The experimental results show that transceiver polarization power imbalance only reduces the signal-to-noise ratio in one polarization, but has little effect on performance of the polarization demultiplexing algorithm with the proposed scheme. In addition, the polarization power imbalance of the transceiver can be monitored simultaneously using frequency domain pilots.**

Keywords—polarization power imbalance, digital subcarrier modulation, polarization demultiplexing

I. INTRODUCTION

Coherent digital subcarrier multiplexing (DSCM) combined with polarization multiplexing is a promising technology for flexible implementation of Point-to-Multipoint (PTMP) network architectures while significantly increasing system capacity [1]. However, in the coherent system with polarization multiplexing, the transceiver imperfections will distort the signal and hence degrade the system performance. Among these, polarization power imbalance (PPI) is one of the impairments introduced by transceiver imperfections. The transmitter (Tx) PPI is mainly caused by polarization fluctuation of input laser, the mismatch of the driving amplifier gain and the optical coupler coupling ratio between the two polarization. The receiver (Rx) PPI may induced by the polarization variation of the local oscillation (LO), mismatch of the output power of balanced detector and the gain of transimpedance amplifier (TIA) between the two polarization. The transceiver PPI will lead to the difference in signal-to-noise ratio (SNR) between the two polarization tributaries depending on their relative orientations [2], resulting in extra margins to guarantee the light path availability [3]. Moreover, it may deteriorate the performance of polarization demultiplexing, and even lead to singularity in the equalization, resulting in the failure of demultiplexing [4].

PPI is a special case of polarization-related loss (PDL), where the power imbalance originates from the transmitter and receiver. The problem relating to PPI in single-carrier systems has been studied extensively [2-5], and similar schemes can be used directly in DSCM systems by regarding the DSCM as multiple single-carrier signals after subcarrier demultiplexing. However, such schemes require repetitive processing of per subcarrier, and the resulting computational redundancy is unacceptable in the power-sensitive short-range applications. In [6], we proposed to joint track the polarization and carrier phase using frequency domain pilot tones (FPT). Polarization demultiplexing for all subcarriers are realized before subcarrier demultiplexing, which greatly reduces the computational redundancy. However, the impact of transceiver PPI has not been investigated. Therefore, schemes to compensate for PPI and polarization aliasing need to be explored for DSCM.

Although the PPI can be compensated, the resulting SNR difference is unavoidable, which will reduce the overall system performance. To mitigate such performance degradation, a possible solution is to monitor the transceiver PPI and maintain the transceiver when the PPI exceeds a certain range. In the single-carrier system, the equalizer coefficients for polarization demultiplexing can be used to estimate the transmitter PPI or receiver PPI [7]. However, the scheme is unable to separate the Tx PPI and Rx PPI when the imbalance is present in both Tx and Rx. In [8], the PPI at Tx and Rx is separated by introducing continuous polarization variation using a polarization scrambler. However, adding a scrambler to the fiber optic link fails to work for systems in service. Therefore, solution for simultaneous monitoring of Tx PPI and Rx PPI is urgently desired for DSCM system in service.

In this paper, a transceiver polarization power imbalance compensation and monitoring scheme for coherent digital subcarrier modulation system is proposed and demonstrated experimentally. In the proposed scheme, two FPTs with different frequencies are placed outside the spectrum of the modulated communication signal. Then FPTs are filter out with a low pass filter (LPF) to realize joint compensation of PPI, polarization aliasing and carrier phase noise. The filtered FPTs are also used to estimate Tx PPI and Rx PPI simultaneously. Experimental results show that transceiver PPI within ± 6 dB has little impact on the performance of polarization demultiplexing. In addition, the proposed scheme can achieve accurate estimation of Tx PPI and Rx PPI in the presence of both Tx and Rx imbalance.

II. PRINCIPLE

Insert a FPT in each polarization separately, the transmitted signal can be expressed as:

$$\begin{bmatrix} E_x(t) \\ E_y(t) \end{bmatrix} = \begin{bmatrix} S_x(t) + Ae^{j\omega_1 t} \\ S_y(t) + Ae^{j\omega_2 t} \end{bmatrix} \tag{1}$$

in which $E_{x/y}(t)$, $S_{x/y}(t)$ denote the transmitted and modulated signals in x/y polarization respectively. A, ω_1 and ω_2 represent the amplitude and angle frequency of the FPTs. The power of the FPT depends on the pilot-to-signal power ratio (PSR), which is defined as $PSR(dB) = 10log10(P_{pilot}/P_{signal})$. P_{pilot} and P_{signal} represent the power of FPT and DSCM signal, respectively.

Considering Tx PPI and Rx PPI, the received signal can be expressed as:

$$\begin{bmatrix} R_x(t) \\ R_y(t) \end{bmatrix} = \boldsymbol{M_{SOP}} \begin{bmatrix} E_x(t) \\ E_y(t) \end{bmatrix} e^{j(\Delta\omega t + \varphi)} + \boldsymbol{n}(t) \tag{2}$$

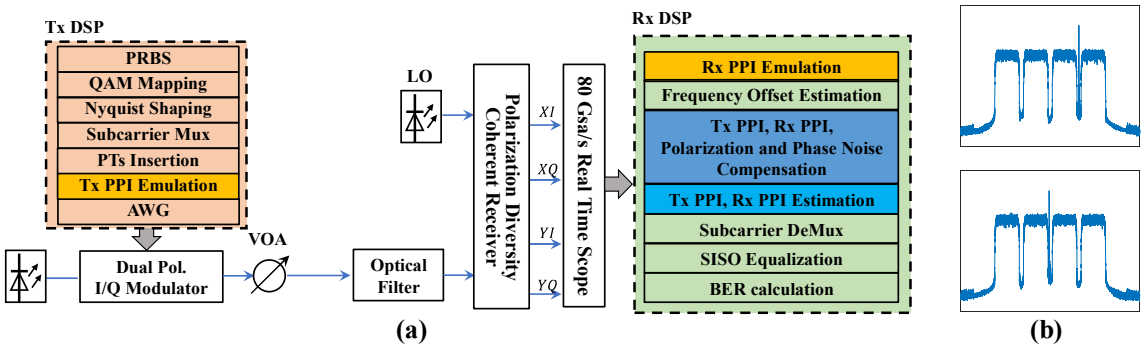

Fig.1: (a) experimental setup and DSP flow; (b) Power spectrum of the transmitted signal

where $R_{x/y}(t)$, $\Delta\omega$, φ, $\boldsymbol{n}(t)$ represent the received signal in dual-polarization, the frequency offset between the signal carrier and the local oscillator, carrier phase noise and additive white Gaussian noise, respectively. $\boldsymbol{M_{SOP}}$ is the matrix describing the Tx PPI, Rx PPI and rotation of state of polarization (RSOP), and $\boldsymbol{M_{SOP}}$ can be expressed as:

$$\boldsymbol{M_{SOP}} = \boldsymbol{H}_{Tx}\boldsymbol{J_{SOP}}\boldsymbol{H}_{Rx} = \begin{bmatrix} m_{11} & m_{12} \\ m_{21} & m_{22} \end{bmatrix} \quad (3)$$

where $\boldsymbol{J_{SOP}} = \begin{bmatrix} cos\alpha e^{j\xi} & -sin\alpha e^{j\eta} \\ sin\alpha e^{-j\eta} & cos\alpha e^{-j\xi} \end{bmatrix}$ is the Jones matrix of RSOP ; $\boldsymbol{H}_{Tx} = \begin{bmatrix} g_t & 0 \\ 0 & 1 \end{bmatrix}$ and $\boldsymbol{H}_{Rx} = \begin{bmatrix} g_r & 0 \\ 0 & 1 \end{bmatrix}$ describe the matrices of Tx PPI and Rx PPI, respectively. The PPI can be described in terms of km as: $G_{Tx/Rx}(dB) = 20log10(g_{t/r})$.

The frequency offset $\Delta\omega$ can be obtained by comparing the received FPT frequency with the transmitted one. Then, the FPTs in X and Y polarization are down-converted to the baseband respectively. A low pass filter is used to filter out the FPTs for estimation of transfer matrix of Tx PPI, Rx PPI, RSOP and carrier phase noise. The transfer matrix $\widehat{\boldsymbol{M}}_{\boldsymbol{SOP}}$ can be obtained as follows:

$$\begin{bmatrix} X_{\omega_1}(t) \\ Y_{\omega_1}(t) \end{bmatrix} = \boldsymbol{H}\left\{\begin{bmatrix} R_x(t) \\ R_y(t) \end{bmatrix} e^{-j(\omega_1+\Delta\omega)t}\right\} = A\begin{bmatrix} m_{11} \\ m_{21} \end{bmatrix} e^{j\varphi} + \boldsymbol{H}\{n(t)\} \quad (4)$$

$$\begin{bmatrix} X_{\omega_2}(t) \\ Y_{\omega_2}(t) \end{bmatrix} = \boldsymbol{H}\left\{\begin{bmatrix} R_x(t) \\ R_y(t) \end{bmatrix} e^{-j(\omega_2+\Delta\omega)t}\right\} = A\begin{bmatrix} m_{12} \\ m_{22} \end{bmatrix} e^{j\varphi} + \boldsymbol{H}\{n(t)\} \quad (5)$$

$$\widehat{\boldsymbol{M}}_{\boldsymbol{SOP}} = \begin{bmatrix} m_{11} & m_{12} \\ m_{21} & m_{22} \end{bmatrix} e^{j\varphi} \quad (6)$$

where $\boldsymbol{H}\{\cdot\}$ represents the LPF operation. $\{\cdot\}^{-1}$ represents the inverse of matrix. $X_{\omega_{1/2}}$ and $Y_{\omega_{1/2}}$ are the FPTs extracted from the X/Y polarization, respectively. In Eq. (6), the constant A is removed after normalization with the total power of the FPT at the corresponding frequency ($\sqrt{|X_{\omega_i}|^2 + |Y_{\omega_i}|^2} = A$). The analysis shows that the estimation of $\widehat{\boldsymbol{M}}_{\boldsymbol{SOP}}$ can be obtained with the help of FPT. This means that the transceiver PPI has little impact on the performance of polarization demultiplexing and carrier phase recovery for the proposed scheme. The matrix $\boldsymbol{T}$ to simultaneously recover the transceiver PPI, polarization aliasing, and carrier phase can be obtained by computing the inverse matrix of $\widehat{\boldsymbol{M}}_{\boldsymbol{SOP}}$: $\boldsymbol{T} = \widehat{\boldsymbol{M}}_{\boldsymbol{SOP}}{}^{-1}$.

After obtaining the estimation matrix $\widehat{\boldsymbol{M}}_{\boldsymbol{SOP}}$, the Tx PPI and Rx PPI can be estimated by:

$$g_r = \sqrt{\frac{|\widehat{M}_{11}||\widehat{M}_{12}|}{|\widehat{M}_{21}||\widehat{M}_{22}|}} \qquad g_t = \sqrt{\frac{|\widehat{M}_{11}||\widehat{M}_{21}|}{|\widehat{M}_{12}||\widehat{M}_{22}|}} \quad (7)$$

where $\widehat{M}_{ij}$ $(i,j \in \{1,2\})$ is the element of matrix $\widehat{\boldsymbol{M}}_{\boldsymbol{SOP}}$. As can be seen from equation (7), Tx PPI and Rx PPI can be estimated simultaneously without interfering with each other.

III. Experience and Result

A. Experiental setup

The proposed scheme is validated experimentally via DP-16QAM DSCM system with 4 subcarrier. The experimental setup and DSP flow is shown in Fig. 1. In the transmitter, the DSCM signals with four subcarriers are generated offline with a total baud rate of 28 GBd, and each subcarrier with a baud rate of 7 GBd. A root-raised-cosine (RRC) filter with a roll-off factor of 0.1 is utilized for pulse shaping. After that, subcarrier multiplexing is implemented with a guard band of 2 GHz between subcarriers, resulting in spectral efficiency of 6.588 bit/Hz. Then, two FPTs are inserted at 9 GHz in the X polarization and -300 MHz in the Y polarization, respectively. The PSR of the FPTs is set to -15dB. The power spectrum of the generated signals is shown in Fig. 1(b). Next, Tx PPI is introduced in the two polarizations. The generated signal is converted to the analog domain via an arbitrary waveform generator and sent to drive the dual-polarization optical IQ modulator. A continuous-wave laser with the linewidth of 100 kHz is fed into the modulator. The modulated signals are launched into 10 km standard single-mode fiber, and a variable optical attenuator (VOA) is used to manage the power.

In the receiver, after coherent detection, a real-time oscilloscope is used to capture the detected signals. The Rx PPI is introduced first in the DSP. The following DSP flow processes the captured signals. Frequency offset is estimated by comparing the frequency of the FPT. Then, the proposed scheme is employed for joint compensation of Tx PPI, Rx PPI polarization, and carrier phase, followed by theTx PPI and Rx PPI estimation. After that, subcarrier demultiplexing is performed. An additional single input single output (SISO) based on direct decision least mean square (DDLMS) with nine taps and the step size of 1e-3 is followed to compensate for inter symbol interference (ISI) and residual phase noise for each polarization. Finally, the BER is calculated.

B. *Compensation of transceiver polarization power imbalance*

First, the transceiver PPI tolerance of the proposed scheme is discussed. In Fig. 2(a), the BER as a function of Tx PPI is investigate in the presence of 2 dB Rx PPI. The Tx PPI is introduced by referring to the high power polarization and reducing the power of the other polarization, and the PPI is defined by $10log_{10}(P_x/P_y)$. As can be seen, significant degradation of the total BER can be observed with increasing of the absolute PPI. However, the BER of the reference polarization state remains at a stable level, and the decrease of total BER is caused by the deterioration of SNR resulting from the power reduction of another polarization. This result illustrates that the Tx PPI has little impact on the performance of polarization demultiplexing for the proposed scheme. The BER as a function of Rx PPI in the presence of -2 dB Tx PPI is also shown in Fig. 2(b). BER remains the same for different Rx PPI. Since loading the Rx PPI in the receiver DSP has no effect on the SNR, the BER difference in X/Y polarization is caused by the SNR difference resulting from the Tx PPI. Next, BER as a function of ROP in the presence of transceiver PPI is given in Figure 2(c) and (d). BER is below the KP4-FEC threshold of 2e-4 when ROP is greater than -18 dBm in the absence of Tx PPI. The same conclusion can be drawn that the transceiver PPI only causes a degradation of the SNR and has no effect on the performance of polarization demultiplexing for the proposed scheme.

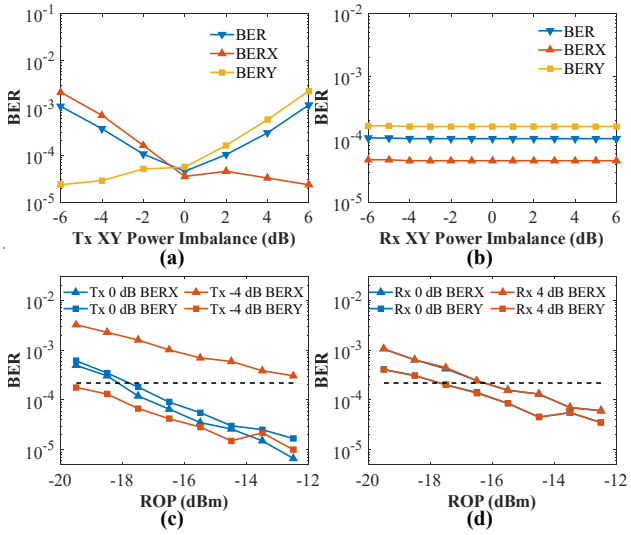

Fig. 2. (a) Tx PPI tolerance with 2 dB Rx PPI; (b) Rx PPI tolerance with 2 dB Tx PPI; (c) BER vs. ROP with 2 dB Rx PPI; (d) BER vs. ROP with -2 dB Tx PPI.

C. *Estimation of transceiver polarization power imbalance*

In this subsection we will analyze the estimated performance of the proposed scheme on the transceiver PPI. The results are shown in Fig. 3. For Fig. 3(a), the Rx PPI is fixed at 2 dB, and the Tx PPI is swept from -6 dB to 6 dB. As can be seen, the estimation error of Tx PPI is within 1 dB and tends to increase with the increase of PPI. One reason for this phenomenon is that the actual Tx PPI differs from the preset value itself due to modulation nonlinearity and nonlinear amplification of the driver. As the absolute value of PPI increases, the difference between the actual PPI and the preset value becomes more significant, leading to the increase of estimation error. In Fig. 3(b), when the Rx PPI sweeps from -6 dB to 6 dB in presence of -2 dB Tx PPI, the estimation error is within 0.1 dB. The small error contributes to that the preset Rx PPI and the actual value are the same.

Subsequently, we analyze the estimated performance of the transceiver PPI under different SNR in Fig. 3(c) and (d). The variation of SNR is realized by sweeping the receiver optical power. In Fig. 3(c), the Tx PPI is estimated with Rx PPI fixed at 2 dB, and in Fig. 3(d), the Rx PPI is estimated with Tx PPI fixed at -2 dB. As can be seen, the proposed scheme maintains the similar estimation performance for different SNR. This is attributed to that the power spectrum of the FPT at the frequency where the FPT is located is much larger than that of the additive white Gaussian noise (AWGN). Therefore, the proposed scheme shows strong robustness to noise and can be used for the estimation of transceiver polarization power imbalance under degradation of severe AWGN.

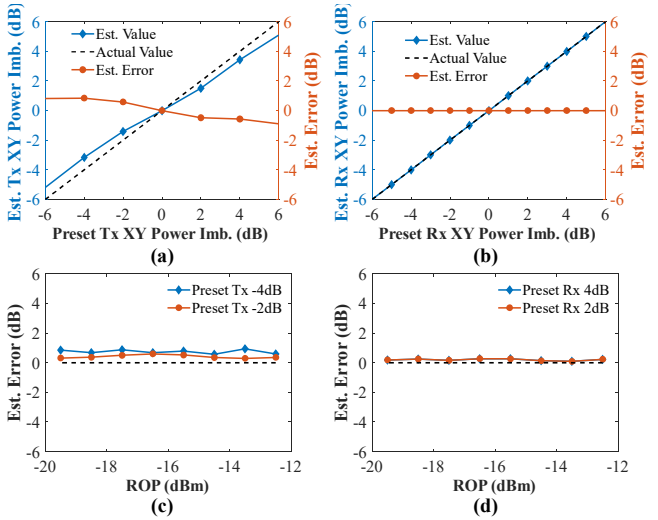

Fig. 3. The estimation of transceiver polarization power imbalance. Estimation of (a) Tx PPI with 2 dB Rx PPI, (b) Rx PPI with -2 dB Tx PPI, (c) Tx PPI with 2 dB Rx PPI under different ROP, (d) Rx PPI with -2 dB Tx PPI under different ROP

IV. CONCLUSION

In this paper, we have proposed a transceiver polarization power imbalance compensation and monitoring scheme using frequency pilot for coherent DSCM system. The scheme can achieve joint compensation of transceiver polarization power imbalance, polarization aliasing, and carrier phase. The proposed scheme is experimentally demonstrated by a 28-GBd DP-16QAM DSCM system with four subcarriers for each polarization. The experimental results show that the transceiver polarization power imbalance within ± 6 dB only degrades the SNR and shows little effect on the performance of polarization demultiplexing after using the proposed scheme. Meanwhile, the proposed scheme is applicable to estimate the polarization power of both Tx and Rx ranged from -6 dB to 6 dB with estimation error less than 1 dB and shows strong robustness to additive white Gaussian noise.

ACKNOWLEDGMENT

This work was supported by Shenzhen Municipal Science and Technology Innovation Council under Grants (JCYJ20190806142407195 and JCYJ20210324131408023)

REFERENCES

[1] D. Welch et al., J. Lightw. Technol. 39(16), 5232-5247, 2021
[2] L. E. Nelson et al., Opt. Express 19(7), 6790-6796, 2011
[3] H. Chin et al., J. Lightw. Technol. 35(4), 931-940, 2016.
[4] L. Lu et al., Proc. ACP, Paper AF2F. 40, 2013.

[5] N. Muga et al., J. Lightw. Technol. 31(13), 2122-2130, 2013.
[6] L. Fan et al., J. Lightw. Technol. 41(5), 1454-1463, 2023.
[7] C. Fludger et al., Proc. ECOC, 2016.
[8] Q. Zhang et al., J. Lightw. Technol. 39(7), 2033-2045, 2021